Model tests on the deformation and collapse processes of small earth dams due to earthquakes and rainfall

H. Nakazawa[1], T. Ishizawa[2], T. Danjo[3], Y. Sawada[4] and Y. Onoue[5]

[1] *Principal Research Fellow, National Institute for Earth Science and Disaster Resilience, nakazawa@bosai.go.jp*
[2] *Chief Researcher, National Institute for Earth Science and Disaster Resilience, ishizawa@bosai.go.jp*
[3] *Research Fellow, National Institute for Earth Science and Disaster Resilience, t.danjo@bosai.go.jp*
[4] *Associate Professor, Kobe University, sawa@harbor.kobe-u.ac.jp*
[5] *Researcher, National Institute for Earth Science and Disaster Resilience, onoue@bosai.go.jp*

Abstract

In recent years, the frequency of disasters because of extreme weather caused by global warming has been increasing, with a consequent increase in related discussions at an international level. However, most research on global warming and climate change have been focusing on phenomena that occur on a global scale; only a few studies have focused on global warming and geotechnical engineering. In particular, it is generally known that soil structures are easily damaged by rainfall or earthquakes. The damage caused by an earthquake may vary according to whether the soil was saturated by rainfall before or after an earthquake. Small earth dams in Japan are particularly prone to damage from earthquakes and rainfall, and many of these require improvement. An energetic safety improvement program is under way. However, as there is currently no effective method to quantitatively evaluate the combined effects of heavy rainfall and earthquakes, it is difficult to define the most appropriate approach to maintenance.

In this study, a series of rainfall experiments and shake table tests using identical models was carried out to confirm that residual deformation and collapse patterns differ depending on patterns of damage preceding rainfall or earthquakes. Two 1/5-scale embankment models of a typical small earth dam in Japan were constructed in rigid soil containers with the same cross section. Then, two simultaneous experiments were conducted: a shake table test using a sinusoidal wave with a maximum acceleration of 224 Gal, which followed a 10-mm/h rainfall experiment using the same model; or a rainfall experiment preceded by a shake table test. A difference in the collapse mechanism and residual deformation of the embankment models due to the order of events was confirmed. It was found that the acceleration response on the upstream side of an embankment was greatly amplified when shaking occurred after preceding rainfall and that the deformation of the model tended to occur at an early stage of shaking. It was also confirmed that the deformation of the embankment models differed depending on the order of rainfall and shaking.

Keywords: small earth dam, rainfall, earthquake, model test, residual deformation

1. Introduction

In recent years, there have been frequent natural disasters because of extreme weather caused by global warming. The impact of climate change on the frequency of natural disasters has been the subject of discussion internationally in both academia and government [1–2]. However, most research on global warming and climate change have been focusing on phenomena that occur on a global scale; only a few studies have focused on global warming and geotechnical engineering and these effects have become non-negligible in recent geotechnical engineering. On the other hand, although earthquakes as a typical disaster may not be related to global warming, they often result in large-scale damage. The seismic design of structures treated in geotechnical engineering has to be upgraded taking into account destructive ground motions that have not previously been considered; for example, earthquakes in combination with excess rainfall or snow, as exemplified by the 2004 Niigata-ken Chuetsu earthquake, which resulted in landslides that were exacerbated by snow [3]. It is known that soil structures are easily damaged by rainfall or earthquakes. Comparing between effects of an earthquake under the condition in which degree of saturation of soil structure has increased due to preceding rainfalls and infiltration by rainfalls occurs after a preceding earthquake conversely, it is expected that the final damage situation such as residual deformations of soil structures will be different each other because these evaluations are depending on a damage state and its level by preceding events just due to the difference in order.

Under thus background, a thorough inspection of small agricultural earth dams was performed over 3 years from 2013 in Japan, examining approximately 96,000 reservoirs, each covering an area greater than 0.5 ha. It was reported that more than 11,000 dams needed to be surveyed in more detail due to the risk of downstream damage to housing if their embankments collapsed. In March 2017, a detailed survey on the earthquake resistance of 4,444 embankments was undertaken. According to this survey, it became clear that 2,434 of these embankments had insufficient earthquake resistance and that 1,399 out of 3,634 locations required countermeasures against heavy rain. In June 2019, it was revealed that if new criteria for disaster prevention were applied to these dams, about 64,000 will have to be improved, which is more than 5 times the number identified in the previous survey. Therefore, a program of safety improvements for embankments is now under way [4]. However, as there are few cases where the combined effects of heavy rain and earthquakes have been quantitatively evaluated, there are difficulties in deciding the appropriate level of maintenance.

The purpose of this study was to confirm that residual deformation and collapse patterns following an earthquake differ depending on the occurrence of preceding rainfall damage. Therefore, 1/5-scale embankment models of a typical small earth dam in Japan were prepared, and a series of rainfall experiments and shake table tests was carried out using these models. This paper reports on the relationship between the dynamic behavior and the residual deformation of embankment models on the one hand and the incidence of rainfall and earthquakes on the other hand.

2. Previous study

There have been many studies that have sought to estimate the impact of rainfall on the seismic resistance of soil structures, such as reservoirs. Recent studies of the seismic performance of small earth dam embankments by Sawada et al. and Nakazawa et al. comprised a series of full-scale experiments [5–7]. Traditionally, a small earth dam with a sloping core zone is adopted as the water leakage method from a reservoir. However, in cases where the quantity of impermeable materials required for this method is insufficient, the use of geosynthetic clay liner (GCL) and bentonite as a water barrier is increasing. Based on this background, the earthquake resistance of an embankment to which GCLs had been applied, its permeability after an earthquake, and the effectiveness of installation methods for GCL sheets were examined. As shown in Fig. 1, although cracks occurred at the crest of the embankment, there was no confirmed water leakage on the downstream side, suggesting that the impermeable sheet remained functional after a shake table test.
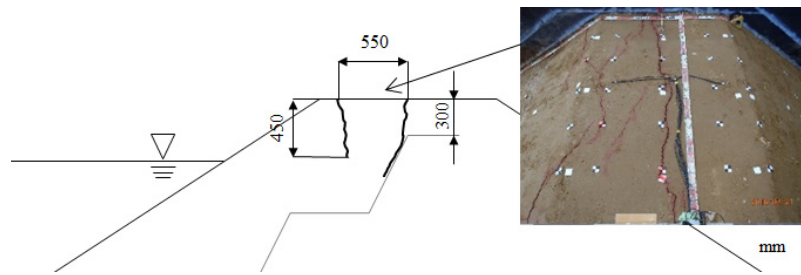
Fig. 1 – Cracks observed after a full-scale model experiment [5]

In addition, there have been several studies on the complex interactions between rainfall and earthquakes by Ichii et al. [7], Matsumaru et al. [8], and Kawajiri et al. [9–10]. For example, Ichii et al. [7] reported an experiment that used an embankment model with a height of 1.2 m to which sinusoidal waves were applied to estimate reductions in the earthquake resistance of the embankment due to rainfall infiltration. The causes of the decline in earthquake resistance in this experiment were a decrease in shear strength due to loss of suction caused by rainfall infiltration and an increase in inertial force due to an increase in unit weight. However, it was difficult to evaluate which of these two factors was most significant. In another experiment by Kawajiri et al., model and triaxial tests were carried out, and the effects of rainfall infiltration into cracks were investigated, to evaluate the reduction in strength of an embankment after an earthquake [9–10]. These studies indicate that cracks increase the permeability of embankments and accelerate the rise of water levels in them. Therefore, it is suggested that a large number of cracks can lead to collapse a dam early during the rainfall.

In this study, a small earth dam was modeled with a reservoir upstream. As shown in field observations of groundwater behavior by Sawada et al. [11], it is thought that the earthquake resistance of small earth dam embankments is lower than that of normal embankments without groundwater because of seepage inside the embankment. On the contrary, there are almost no experimental studies on the complex effects of rainfall and earthquakes on small earth dams that use embankment models with a reservoir on the upstream side.

3. Outline of model tests

This chapter outlines the series of experiments carried out in this study. In previous studies, the seismic resistance of small earth dams was verified using full-scale embankments but not estimated the influence caused by heavy rain. However, there is no method to quantitatively evaluate the combined influence of heavy rainfall and earthquakes on embankments. However, it is difficult to improve the design and maintenance methods for embankments to take into account measures against both heavy rainfall and earthquakes.

In this study, a series of rainfall and shake table tests using an identical model was carried out to confirm that residual deformation and collapse patterns differ depending on patterns of prior rainfall and earthquakes.

3.1 Experimental model

In a series of experiments, two identical embankment models with reservoirs were constructed in 1.5-m high, 1.0-m wide, and 4.0-m long rigid soil containers. The model on the left in Fig. 2 details the effects of preceding rainfall (Case A), whereas the model on the right illustrates the effects of a preceding earthquake (Case B). The model was scaled down to one-fifth of a full-scale experimental model with reference to experiments by Sawada et al. (2016; 2018). Drainpipes were installed in each section so that the water level in the reservoir was kept constant during rainfall experiments. Measurement sensors, including

3

accelerometers, pore water pressure gauges, and deformation transducers, for shake table tests and soil moisture and earth pressure meters for rainfall experiments were installed in the model.
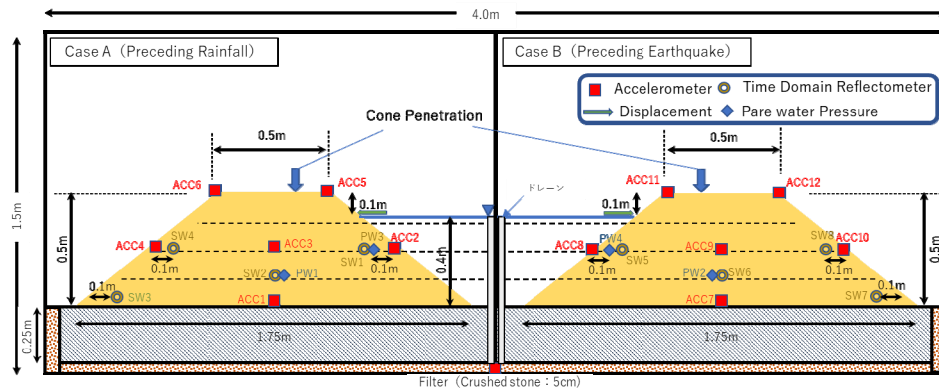
Fig. 2 – Cross section of embankment models with reservoirs

3.2 Experimental device and materials

A series of experiments were performed in the large-scale earthquake simulator at the National Research Institute for Earth Science and Disaster Resilience, Tsukuba, Japan. The features of this facility are presented in Table 1. Fig. 3 shows the shake table arrangement. As indicated in Table 1, the shake table measures 14.5 × 15.0 m (with a load area of 12.0 × 12.0 m), the maximum load capacity is 4,900 kN, the acceleration is approximately 0.5 G (490 Gal) with a load of 4,900 kN and approximately 0.8 G (784 Gal) with load of 2,450 kN, and the stroke is ±22 cm.

Table 1 – Shake table specifications

Loading capacity	500 ton
Table size (area)	14.5 m × 15 m (217.5 m^2)
Shaking direction	Horizontal, 1-dimensional
Maximum acceleration	940 cm/s^2 for 200 ton
	500 cm/s^2 for 500 ton
Maximum velocity	100 cm/s
Maximum displacement	±22 cm

Photo 3 shows the appearance of the sprinkler for the rainfall test. This device has a structure that straddles the outer shape of the soil container used in the experiment and can generate uniform rainfall within an area of 1 × 1.8 m. The watering mechanism is a system in which 500 rain needles are vibrated by a motor, generating rain from a height of 2.0 m above the soil container. The raindrop diameter is variable in the range of ϕ1.7 to 3.0 mm, and the rainfall intensity can be controlled in the range of 10 to 80 mm/h.

4

(a) Complete view of the shake table   (b) Rainfall sprinkler device and soil container

Fig. 3 – The shake table and experimental situation

The geotechnical material used in this experiment was cultivated soil, sampled from Ibaraki Prefecture, Japan, and classified as a volcanic ash. Fig. 4 illustrates the particle-size distribution curve and Table 2 presents the physical properties of the soil. The soil was mostly composed of sand and silt, and the plasticity index, I_p, was 9.9, which indicates low plasticity. Before the construction of the embankment model, this material was in a highly heterogeneous state. The natural water content, w_c, was 45.3% in the silt and 4.4% in the sand mass where the sand content was considered to be dominant.
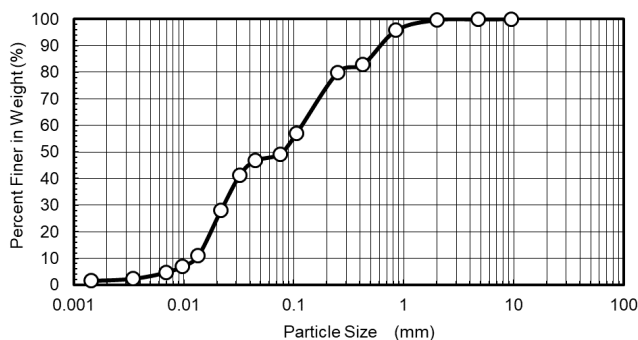
Table 2 – Chemical composition of cement samples

Fig. 4 – Grain size distribution

Density of soil particles	ρ_d	(g/cm^3)	2.634
Maximum grain size	D_{max}	(mm)	9.5
Fine content (<0.075 mm)	F_c	(%)	49.3
Mean particle size	D_{50}	(mm)	0.077
Uniformity coefficient	U_c		9.475
Optimum water content	w_{opt}	(%)	23.4
Maximum density	ρ_{dmax}	(g/cm^3)	1.499
Liquid limit	ρ_{dmax}	(%)	43.2
Plastic limit	ρ_{dmax}	(%)	33.3
Plasticity index	I_p		9.9

3.3 Construction of the experimental model

As shown in Fig. 2, the embankment on the foundation, which was 0.25-m thick using the same ground material as the model, was designed to have a shape 0.5 m in height, 0.5 m in width at the top with a slope of 1.25:1. By dividing the embankment into four layers such that the density of each layer was uniform to control the density of the embankment model, two embankments with the same cross section were constructed. In this experiment, modeling of the sloping core of a standard earth dam was omitted to simplify the experimental conditions. After the construction of the two models, water was injected into the center space of both models to form a reservoir with a depth of 0.4 m. In addition, a filter layer made of crushed stone corresponding to gravel was installed at the bottom of the soil container, as shown in the cross section. PVC pipes adjusted to the water surface height were connected to the filter layer to provide drainage, preventing water level changes during rainfall.

As described in the next section, the model on the left side in Fig. 2 represents the case of preceding rainfall (Case A) and the model on the right side represents the case of a preceding earthquake (Case B). The

5

homogeneity of the embankment models in both cases was confirmed by a lightweight dynamic cone penetration test [12]. According to the results shown in Fig. 5, although the cone resistance q_d in the surface layer at 10 cm is slightly lower, the entire embankment model indicates a uniform q_d distribution in both cases. Table 3 shows the conditions of the embankment models after construction. It was determined that the wet densities rt of the embankment models should be set at a low level to allow for easy reproduction of the damage in the experiment. Consequently, rd values after construction were 1.53 t/m³ for Case A and 1.48 t/m³ for Case B.
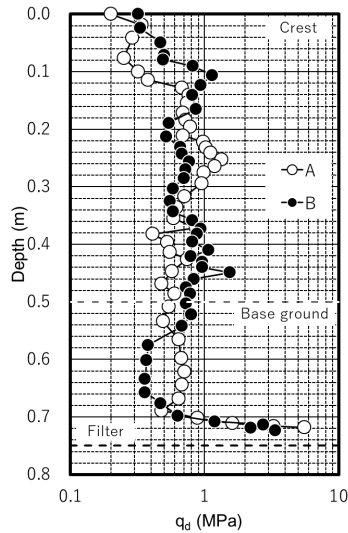

Fig. 5 – Results of lightweight dynamic cone penetration tests

Table 3 – Condition of embankment model

	Wet density ρ_t (t/m³)	Water content	
		After construction w_c (%)	After experiment w_c (%)
Case A	1.53	45.3	55.5
Case B	1.48	35.1	50.3

3.4 Experimental cases and conditions

As shown in Table 4, the model experiments, including two shake table tests after preceding rainfall (Case A) and a rainfall test after preceding shake table tests (Case B), were performed simultaneously to confirm the difference in damage caused by different patterns of earthquakes and rainfall. The experiment included the following tests: a rainfall test for Case A, shake table tests with three stages of acceleration for both cases, a rainfall test for Case B, and finally shake tests with three stages of acceleration for both cases.

The rainfall experiment involved rainfall of 10 mm/h for about 10 min, and the input accelerations were targeted for 50, 100, and 150 Gal. With respect to the waveform, a 3-Hz sinusoidal wave of 2 s for each of the gradually increasing and decreasing portions was applied to the shake table for 8 s. As a result, the actual accelerations acting on the shake table and at the bottom of the model were, respectively, 75, 155, and 224 Gal for nos. 2 to 4, and 81, 154, and 226 Gal for nos. 6 to 8.

4. Results

A series of experimental data are summarized, followed by the results, focusing on the shake table tests, to explain residual deformations due to difference between rainfall and earthquake.

4.1 Overview of experimental results

Fig. 5(a) and (b) show the timing of each test from the start to the end of the series of experiments and the changes in data obtained by the soil moisture meter shown in Fig. 2. Because the data measured by the soil moisture meter are displayed as voltage values, not saturation degrees, they only show permeation characteristics. A positive change in this data means that the degree of saturation inside the embankment model has increased.

6

Table 4 – Experimental cases and events

No.	Case A	Case B	Event
1	Rainfall of 10 mm/h (about 10 min)	—	Erosion occurred on the slope of Case 1.
2	Shaking by sinusoidal waves with 75-Gal acceleration		No deformation or damage in both cases.
3	Shaking by sinusoidal waves with 155-Gal acceleration		Erosion on the upstream slope of Case 1 occurred due to ripples in the reservoir caused by sinusoidal waves.
4	Shaking by sinusoidal waves with 224-Gal acceleration		—
5	—	Rainfall of 10 mm/h (about 10 min)	Movement of the sliding soil mass upstream from Case 2 progressed due to rainfall infiltration into the crack at the crest.
6	Shaking by sinusoidal waves with 81-Gal acceleration		—
7	Shaking by sinusoidal waves with 154-Gal acceleration		
8	Shaking by sinusoidal waves with 226-Gal acceleration		Observation of residual deformation after drainage confirmed that the embankment as a whole in Case 1 was deformed upstream and that in Case 2 there was a further movement of the sliding soil mass caused by the preceding earthquake.

Based on each time segment shown on the horizontal axis of Fig. 6, the contour diagrams of voltage value of Case A are shown as an example. At 12:42, which is the display start time in the figure, water was injected into each reservoir until filled as planned. In Case A, during the preceding rainfall indicated at (1), it was confirmed that the voltage values of SW 1 to 3 did not change because the seepage line had already been formed on the upstream side. However, the increased in the voltage value due to rainfall infiltration in SW4 installed in unsaturated layer on the downstream side can be confirmed. Then, until the shake table tests were started, the voltage values of both Case A and B were almost constant, and there was little change in the degree of saturation in the embankment models. After that, in a series of shake table tests indicated at (2) to (4), the voltage increase in Case B was more than that in Case A after the test (4) by the acceleration of 224 Gal at (4). The remarkable increase in SW5 voltage on the upstream side suggests that the absence of rainfall infiltration promotes the change in water content in the embankment model.
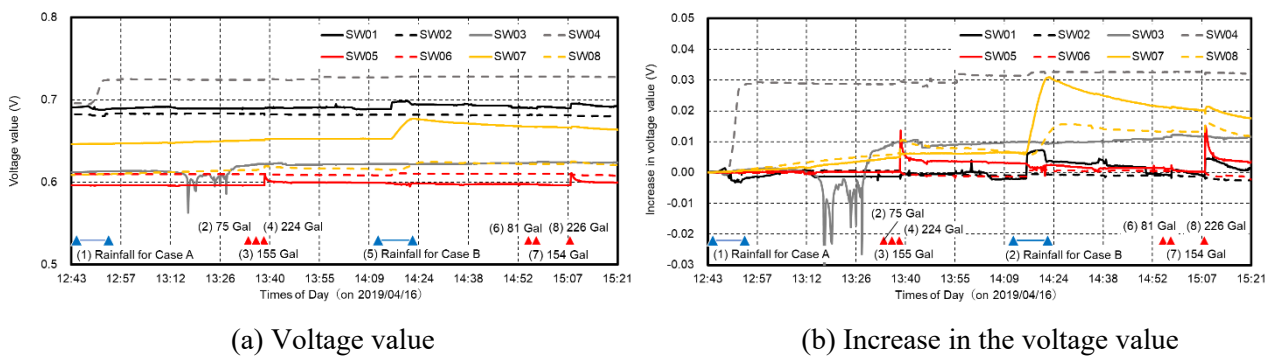

(a) Voltage value

(b) Increase in the voltage value

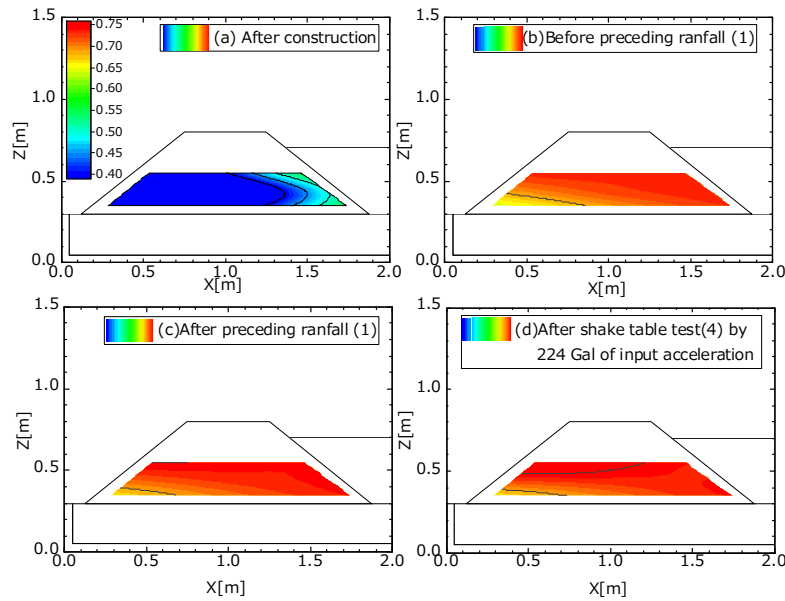Fig. 5 – Progress of voltage values

7

Fig. 6 – Contour diagrams of voltage values in Case A

4.2 Results of shake table tests

In Case A with preceding rainfall, a series of shake table tests (2 to 4, as shown in Table 4) were performed without any deformation of the embankment model because of factors other than rainfall erosion. Under acceleration between 75 and 155 Gal, no deformation of the embankment models was observed, and the acceleration responses differed little between Cases A and B regardless of the preceding rainfall. In the shake table test with an acceleration of 224 Gal, serious damage occurred as shown in Fig. 7(a) to (c), especially the horizontal displacement of the embankment model of Case A increased with shaking. In relation to pore water pressure, though Case A showed negative pressure, it can be confirmed that excess pore water pressure was generated at the same time as shaking in both cases.
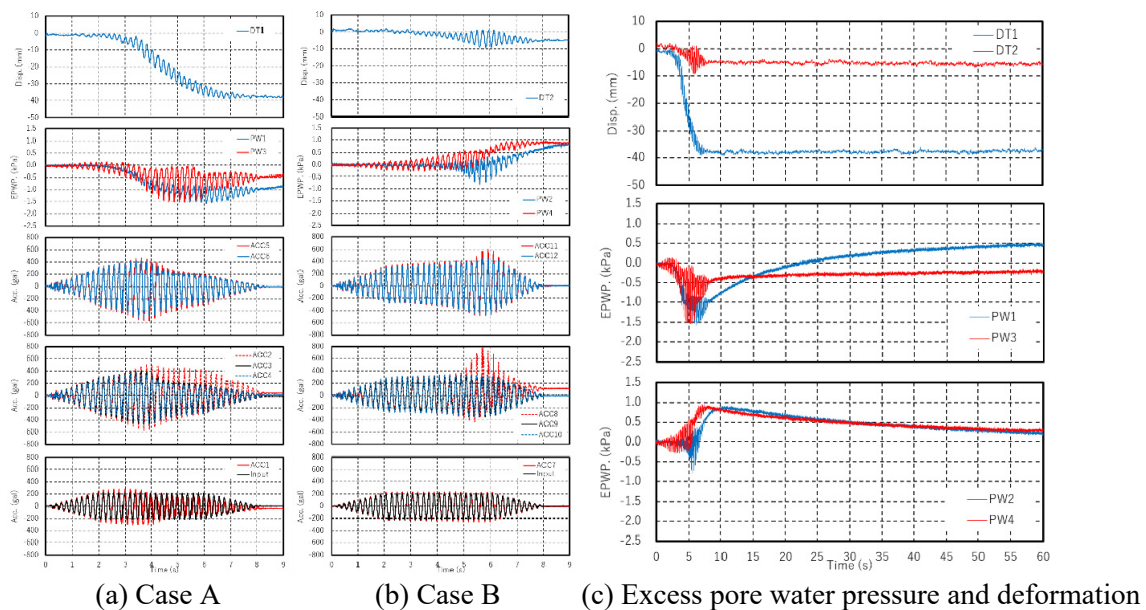

(a) Case A   (b) Case B   (c) Excess pore water pressure and deformation

Fig. 7 – Time histories of shake table tests at 224 Gal after preceding rainfall experiments

8

Looking at ACC5 and 6 in Case A and ACC11 and 12 in Case B, shown in Fig. 2, installed at the shoulders of the embankments, the acceleration response in Case A was amplified until $t = 4$ s and then attenuated. On the contrary, in Case B, it was amplified with a peak indicated at $t = 6$ s and then shifted. This tendency of Case B was remarkable in ACC8. Therefore, it is believed that a crack occurred in the crest of the embankment model at this point and a sliding failure occurred toward the downstream side, as shown in Fig. 8. In addition, although no cracks were observed in Case A, a large deformation occurred below the water level of the reservoir. Fig. 7(c) shows changes in the horizontal displacement of the embankment model and the excess pore water pressure after shaking. It can be seen that the dissipation of excess pore water pressure recovered slowly after shaking. However, horizontal displacement occurred during shaking and changed little after the shaking test.
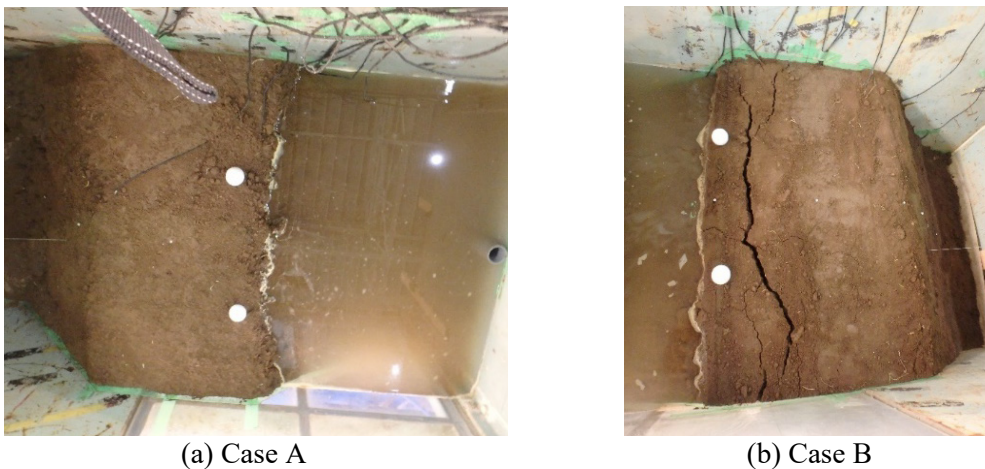

(a) Case A   (b) Case B

Fig. 8 – Situations at the crests of the embankment models after 224-Gal shaking

Subsequently, in the tests 6 to 8, as shown in Table 4, it was confirmed that excessive pore water pressure combined with shaking at 154 Gal was different each other between Case A and B, although dynamic behaviors in both cases indicated almost no difference under shaking at 81 Gal. Focusing on the results at 226 Gal shown in Fig. 9(a) to (c), the acceleration response of ACC2 installed on the upstream side shows a peak at $t = 2$ s in Case A and at $t = 6$ s at ACC8 in Case B. The tendency of the excess pore water pressure was similar to the results in tests 2 to 4 shown in Table 4. In both cases, the excess pore water pressure was generated simultaneously with shaking, and Case A showed negative pressure. Regarding the horizontal displacement of the embankment models, displacement only occurred during shaking and no deformation or no progress of deformation could be observed after shaking regardless of the excess pore water pressure, according to Fig. 9(c).

Based on these results, we found that the dynamic response characteristics of an embankment model differ depending on the preceding event (earthquake or rainfall), although the failure mechanisms are different in Cases A and B. If an earthquake occurs after saturation of the embankment, or the seepage line rises due to preceding rainfall, it is thought that the deformation of the embankment model occurs due to a decrease in shear resistance. Conversely, if an earthquake precedes rainfall, it is suggested that the shear strain and cracks generated due to the earthquake make it easy for rainfall to penetrate the embankment model. Consequently, it is thought that this phenomenon causes a collapse of the embankment slope toward the upstream side.
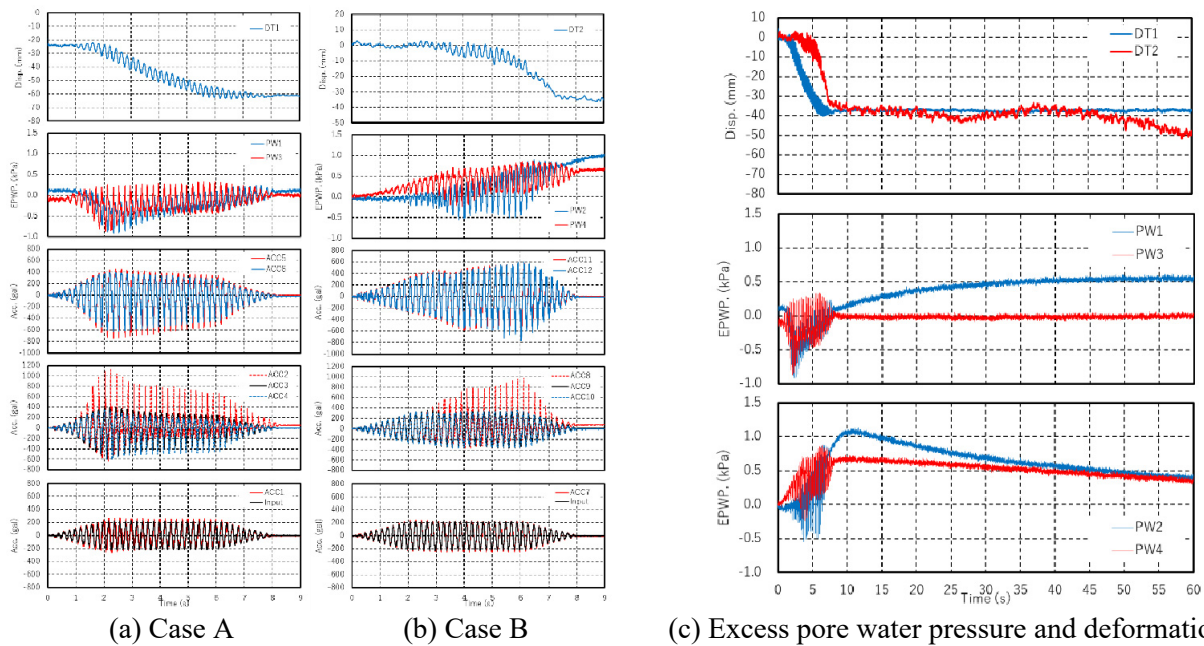
9

(a) Case A   (b) Case B   (c) Excess pore water pressure and deformation

Fig. 9 – Time histories of shake table tests at 226 Gal after shake table tests and rainfall experiments

5. Influence of rainfall and earthquakes on residual deformation

Fig. 10 shows the deformation of embankments after preceding rainfall and subsequent shaking in Case A and after a preceding earthquake and the rainfall experiment in Case B, containing the initial shape after embankment construction and after water injection into each reservoir part. To compare the deformation in both cases easily, the Case A illustration is reversed left to right in Fig. 10(a). Although it is difficult to observe the slope shape on the upstream side after water injection, in Case A, which was subject to preceding rainfall, a wide range of deformation were seen from the center of the crest and shoulder of the embankment model on the upstream side. On the contrary, in Case B, which was affected by a preceding earthquake, cracks near the front shoulder on the upstream side were caused by shaking before the rainfall experiment. This damage suggests the occurrence of a local sliding failure toward the upstream side. However, the effect of subsequent rainfall was not noticeable.

Fig. 11 shows the residual deformation after drainage from the reservoir sections in both cases and indicates that the deformation shown in Fig. 10 became even more noticeable. Fig. 12 shows the residual deformation photographed at the crest of the embankments after final drainage. In Case A, because fine tension cracks were observed at the crest, it is suggested that extensive deformation occurred throughout the embankment. On the contrary, according to the residual deformation in Case B, it is probable that the initial slip soil mass, which had already been generated by the preceding earthquake, was moved further toward the upstream side by the final shake table tests after the rainfall experiment.
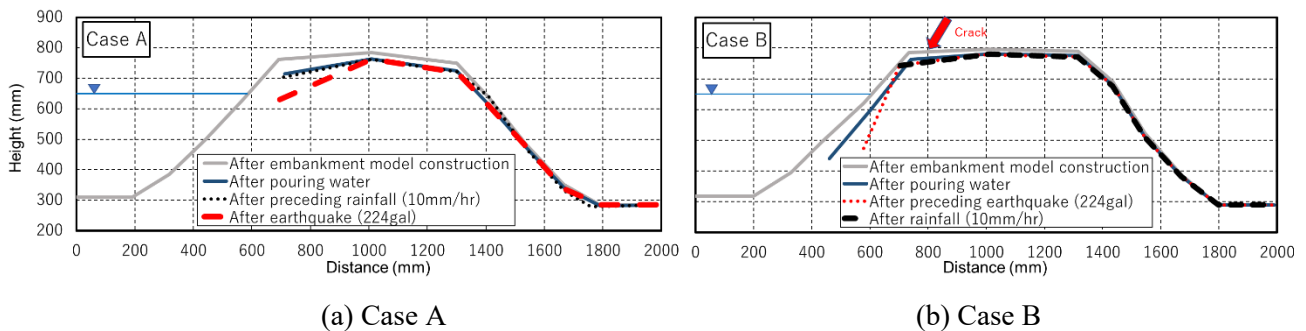
10

(a) Case A   (b) Case B

Fig. 10 – Deformation caused by both shaking and rainfall

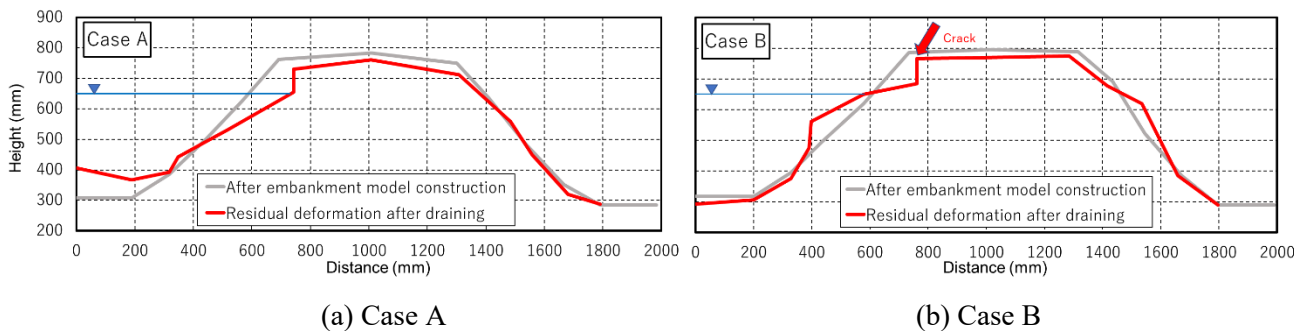(a) Case A   (b) Case B

Fig. 11 – Residual deformation

(a) Case A   (b) Case B

Fig. 12 – State of the embankments after drainage (with the reservoir sections on the left side)

6. Summary

In this study, differences in the residual deformation of small earth dam embankments due to different order of earthquakes and rainfall were confirmed through shake table tests and rainfall experiments. The following observations were made from a series of experiments: 1) Where there was shaking after preceding rainfall, the acceleration response on the upstream side of the embankments was greatly amplified, and the deformation of the model tended to occur at an early stage of shaking. 2) It was confirmed that deformation of the embankment models differed depending on the order of rainfall and shaking. 3) According to the final shake table testing after both rainfall and shaking, it was confirmed that the deformation of the embankments during shaking became stronger and more noticeable.

It is considered that there might be no effective countermeasures against a simultaneous earthquake and rainfall because of the rarity of both events occurring at the same time. Although the results of this experimental study do not show the infiltration process into the embankment model due to rainfall, it is suggested that the effect of changes in the degree of saturation on seismic resistance was evident. Therefore, it is of value to estimate the changes in the degree of saturation and the seepage line inside the embankment in detail.

7. Acknowledgments

8. References

[1] Ministry of the Environment (2014): Results considering the uncertainty of climate change prediction in Japan, Japan Meteorological Agency press release, http://www.env.go.jp/press/files/jp/25606.pdf (accessed on January 30, 2020, in Japanese)

[2] Intergovernmental Panel on Climate Change (2014), Climate change 2013 (translated by Japan Meteorological Agency), http://www.data.jma.go.jp/cpdinfo/ipcc/ar5/ipcc_ar5_wg1_ts_jpn.pdf (accessed on January 30, 2020, in Japanese)

[3] Chigira M (2011): Slope collapse, *Geology and Survey*, **128**), 9-14. (in Japanese)

[4] Ministry of Agriculture, Forestry and Fisheries (2017): Implementation status of detailed surveys based on simultaneous inspection of small earth dams (as of March 31, 2017), http://www.maff.go.jp/j/press/nousin/bousai/170922.html (accessed on June 22, 2019, in Japanese)

[5] Sawada Y, Nakazawa H, Oda T, Kobayashi S, Shibuya S Kawabata T (2018): Seismic performance of small earth dams with sloping core zones and geosynthetic clay liners using full-scale shaking table tests, *Soils and Foundations*, **58** (3), 519-533.

[6] Sawada Y, Nakazawa H, Take WA, Kawabata T (2019): Full scale investigation of GCL damage mechanisms in small earth dam retrofit applications under earthquake loading, *Geotextiles and Geomembranes*, **47**(4), 502-513.

[7] Ihcii K (2005): Experimental study on seismic resistance reduction of embankment due to rainfall, *Proceedings of the JSCE Earthquake Engineering Symposium*, **28**, https://doi.org/10.11532/proee2005a.28.188 (in Japanese)

[8] Matsumaru T, Kojima K, Tateyama M (2014): Fundamental research about seismic behavior of embankment affected by seepage water, *Journal of Japan Society of Civil Engineers*, Ser. C (Geosphere Engineering), **71** (1), 135-149. (in Japanese)

[9] Kawajiri S, Nunokawa O, Itoh Y, Nishida M, Matsumaru T, Kawaguchi T, Ota N, Sugiyama T (2014): Experimental study of embankment collapse mechanism due to rainfall after earthquake, *Japanese Geotechnical Journal*, **9** (2), 153-168 (in Japanese)

[10] Kawajiri S, Nunokawa O, Ota N (2015): Influence of crack on water behavior on embankment due to rainfall, *Journal of Japan Society of Civil Engineers*, Ser. C (Geosphere Engineering), **71** (3), 204-217. (in Japanese)

[11] Sawada Y, Maki R, Kaminobu K, Tanimoto M, Nakazawa H, Kawabata T (2019): In Situ Water Level Measurement in a Small Earth Dam Repaired with Geosynthetic Clay Liners, *Irrigation, Drainage and Rural Engineering Journal*, **87** (2), I_357-363. (in Japanese)

[12] Langton DD (1999): The Panda lightweight penetrometer for soil investigation and monitoring material compaction, *Ground Engineering September*, 33-34.